DOI: 10.1002/chem.200600027

Mechanisms of and Effect of Coadsorption on Water Dissociation on an Oxygen Vacancy of the MgO(100) Surface

Yan Wang,[a, b] Hung N. Nguyen,[a] and Thanh N. Truong*[a]

Abstract: The dissociation mechanism of a water molecule at an oxygen vacancy on the MgO(100) surface was studied by using the embedded cluster method at the DFT/B3LYP level, while the energetic information was refined by using the IMOMO method at the CCSD level. We found that a water molecule initially adsorbs on one of the magnesium ions surrounding the vacancy site with a binding energy of 15.98 kcal mol^{-1}. It then can dissociate on the MgO(100) surface along two possible dissociation pathways. One pathway produces a hydroxyl group bonded to the original magnesium with a proton filling the vacancy via a transition state with a barrier of 4.67 kcal mol^{-1} relative to the adsorbed water configuration. The other pathway yields two hydroxy groups; the hydroxy group originally belonging to the water molecule fills the vacancy, while the hydrogen atom binds with the surface oxygen to form the other hydroxy group. Hydrogen atoms of these hydroxy groups can recombine to form a hydrogen molecule and the surface is healed. Although the barrier (14.09 kcal mol^{-1}) of the rate-controlling step of the latter pathway is higher than that of the former one, the energies of all of its stationary points are lower than that of the separated reactants (H_2O + cluster). The effects of water coadsorption are modeled by placing an additional water molecule near the active center, which suggests that the more coadsorbed water molecules further stabilize the hydroxy species and prevent the hydrogen molecule formation through the latter pathway. The results support the photoemission spectral evidence of water dissociation on the defective MgO(100) surface at low water coverage.

Keywords: density functional calculations · MgO surface · surface chemistry · water coadsorption · water dissociation pathway

Introduction

The dissociation of water on MgO surfaces plays important roles in many chemical processes involved in surface science, environmental chemistry, and bioengineering and, thus, has received considerable attention.[1–15] Previous experiments have shown that its dissociation mechanism is complex and can be affected by the quality of the surface as well as by water vapor pressure and surface temperature.[16–20] Particularly, photoemission spectra, infrared spectra, and low-energy electron diffraction (LEED) data showed the considerable signatures of hydroxy groups (dissociated products) on the defective MgO surface, namely on vacancies or steps on cleaved surfaces.[21,22] It is a well-accepted fact from previous experimental and theoretical studies that the point defects such as oxygen vacancies on the MgO surface in addition to structural defects such as steps and kinks facilitate the water dissociation.[22–28] However, the detailed reaction mechanism of water dissociation on the oxygen vacancy is still not well understood.[13] For example, synchrotron-based photoemission spectroscopy and LEED experiments have recently detected 5% monolayer coverage of hydroxy groups produced through water dissociation on the perfect MgO(100) surface at $p(H_2O) \leq 2 \times 10^{-5}$ Torr and 35% monolayer coverage of that on the Ar^+-sputtered MgO surface, which has a high concentration of oxygen vacancies.[22] Photoemission data also suggested that water dissociation on the perfect surface requires significantly more activation energy than on the point defects of an MgO surface.[29] In contrast, Goodman and co-workers found no evidence for the dissociation of water on the defective MgO surface in their temperature-programmed desorption (TPD) and metastable impact electron spectrosco-

[a] Dr. Y. Wang, H. N. Nguyen, Prof. T. N. Truong
Henry Eyring Center for Theoretical Chemistry, Department of Chemistry, University of Utah
315 S. 1400 E, Room 2020, Salt Lake City, UT 84112 (USA)
E-mail: truong@chem.utah.edu

[b] Dr. Y. Wang
On leave from Department of chemistry, Beijing Normal University, Beijing 100875 (P. R. China)

py (MIES) experiments.[30–32] Therefore, the experimental detection of hydroxy groups exhibits a strong dependence on the measurement conditions as well as on the surface preparation, demonstrating the complex mechanisms of water dissociation on surface defects.[22,31–34] The ambiguity regarding the mechanism of water dissociation on the defective MgO surfaces still persists.[35]

The adsorption of a water molecule on a defective MgO surface has also been examined in a number of theoretical studies. Calculated thermodynamics data have suggested that the dissociation of water on defective MgO surfaces is affected by, for example, the water–surface orientation[36–38] and the coadsorbed water.[25,39,40] Ahlswede et al.[41] used the MSIINDO semiempirical method to calculate the adsorption energies of H, OH and H+OH species on the defects, and concluded that dissociative adsorption would take place at the surface point defects, such as Fs (oxygen vacancy) and Ms (di-oxygen vacancy) centers. Using molecular-dynamics simulations based on the pseudopotential plane-wave DFT approach, Finocchi et al.[7] suggested a different dissociation pathway in which the oxygen atom of the water heals the surface, that is, $H_2O(ad) \rightarrow H_2(g) + O(surface)$. However, these results were derived from constraint MD simulations. The actual potential energy surface along such a pathway has not been identified. In addition, these theoretical studies[7,41] only examined the adsorption of isolated water. In our previous study[42] we have shown that the coadsorption of at least one additional water molecule (water dimer) is sufficient to observe water dissociation on the perfect MgO surface. Therefore, one can expect that coadsorption would play an important role in stabilizing the hydroxy species on the surface and thus would be crucial for understanding the mechanism of water dissociation on an oxygen vacancy on the MgO(100) surface.

In this study, our main objective is to determine the possible dissociative pathways of water on an oxygen vacancy on the MgO(100) surface. In particular, the roles of coadsorption in the dissociative mechanism, which have not been addressed previously, will be a focus of this study. To be able to make comparisons with our previous work on the dissociative adsorption of water dimer on the perfect MgO(100) surface,[42] we used the same level of electronic structure theory to examine the potential energy surface of isolated water and water dimer adsorbed on an oxygen vacancy of an MgO(100) surface. In addition, the theoretical analysis of spectral properties of water dissociation with respect to those of analogous species in experiments is used to explain or support experimental observations.

Computational Methods

The interaction of H_2O with the surface oxygen vacancy of MgO(100) is studied by using the embedded cluster approach. To represent a surface oxygen vacancy (Fs center) in this approach, the surface oxygen atom in the center of the MgO(100) surface is removed to create the $Mg_{21}O_{12}$ cluster (Figure 1). This cluster is treated quantum mechanically along with the adsorbate (isolated water molecule or water dimer), and surrounded by a set of total ion model

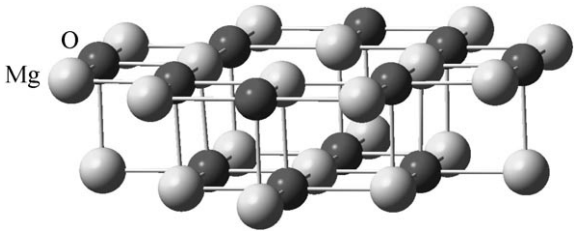

Figure 1. Cluster model $Mg_{21}O_{12}$ with an oxygen vacancy in the surface center.

potential (TIMP) for all Mg^{2+} ions that are nearest to any quantum oxygen atom and a set of point charges whose unit cell was within 1.2 nm from any of the quantum cluster atoms. These TIMP and point charges (PC = ±2) are located at the lattice positions, which were taken from the experimental MgO bulk structure. With these TIMPs, the artificial polarization of oxygen anions at the cluster borders can be reduced and orthogonality of the cluster orbitals to orbitals of the crystal surrounding can be approximated.[43,44] The Madelung potential from the remaining extended MgO surface is represented classically by a set of surface charges derived from the surface charge representation of the external embedding potential (SCREEP) method.[45] More details on the SCREEP method can be found in references [42,45–48].

The hybrid B3LYP DFT method was used with a mixed basis set to calculate the dissociation reactions of water. The 6–311G(d, p) basis set was used for the water molecule, and the 6–31++G(d, p) basis set was used on the Mg atoms nearest the vacancy to describe the electron localization in the cavity. The 6–31G(d, p) basis set was used for the four nearest neighbor surface O atoms surrounding the oxygen vacancy. The 3–21G(d, p) basis set was used for the remaining cluster atoms.

Geometries of the adsorbed isolated water molecule and selected geometrical parameters of the MgO quantum cluster are fully optimized in determinations of all stable and saddle-point structures for the water dissociation paths on the oxygen vacancy. In particular, the surface atoms surrounding the vacancy site, that is five Mg atoms and four O atoms were fully relaxed. Normal mode analyses were done to confirm the nature of each stationary point. In the case of the water dimer, we are mainly interested in the effects of water coadsorption on the dissociative pathways. Thus, at each stationary point on the dissociative pathways of the isolated water adsorption on the oxygen vacancy, the geometry of the coadsorbed water is fully optimized, while the geometries of the dissociated water molecule and the MgO cluster are fixed from the isolated water case.

To improve the energetic properties, we also employed the IMOMO (integrated molecular orbital + molecular orbital) method.[49,50] The IMOMO method allows interactions

in a subregion of the system to be treated at a more accurate level of theory and thus provides a cost-effective method for improving energetic properties in our previous studies of adsorption on metal oxide surfaces.[42,47,48] In this case, a smaller quantum cluster consisting of the adsorbed water and nine atoms surrounding the vacancy was selected as a model system, and was treated at the CCSD level with the above mixed basis set. Hereafter, all energies referred to in this study are at the IMOMO theory level. The interaction energies have been corrected by the basis set superposition error (BSSE) using the counterpoise method within the IMOMO formulation for calculating the total energy.[51] All calculations were carried out by using the Gaussian03 program.[52]

Results and Discussion

Electronic structure of the oxygen vacancy on the MgO(100) surface: It is known that an oxygen vacancy on the MgO-(100) surface (Fs center) is energetically the most stable point defect compared to other kinds of point defects.[13] A detailed description can be found in our previous study.[53] The surface relaxation surrounding the oxygen vacancy is small, comprising outward movements of the nearest four Mg atoms on the surface by 4.7% and the next shell O atoms by 2.4%. Similar relaxation of 4–8% was observed for a bulk F^+ center from EPR experiments.[54] The calculated electron density distribution shows a significant electron density localized in the vacancy region, which has been discussed in our previous work.[53] The formation energy of the vacancy calculated with respect to a free oxygen atom in its ground state is equal to 207.5 kcal mol^{-1} with the BSSE correction, which also is consistent with the experimental estimate of 158~227 kcal mol^{-1}.[55–58] These results indicate that the embedded cluster model and the level of theory used in this study are sufficiently accurate to describe the oxygen vacancy MgO(100) surface.

Adsorption of isolated water on an oxygen vacancy of the MgO(100) surface: For the adsorbed water state, we fully optimized the geometry of the adsorbed H_2O molecule and the nine atoms surrounding the vacancy site. Selected geometrical parameters of the adsorbed water molecule are given in Table 1. Consistent with the periodic simulation results of Finocchi et al.,[7] the adsorbed water is aligned nearly parallel with the two hydrogen atoms tilting slightly toward the surface vacancy. In particular, the oxygen atom of H_2O is almost on top of the magnesium atom (Mg1) next to the vacancy with the O5–Mg1 distance of 2.27 Å; the hydrogen atom H6 forms a hydrogen bond with a nearest surface oxygen atom (O2); the H6–O2 distance is 1.91 Å. The other hydrogen atom (H7) points towards the vacancy and the H7–Fs distance is 2.26 Å. Thus the H7–Fs bond is 0.35 Å longer than H6–O2 bond, which results from the adsorbed water molecule being repulsed slightly by the electrons around the vacancy site. The calculated binding energy is 15.98 kcal mol^{-1} by using the IMOMO (CCSD:B3LYP) method with inclusion of the BSSE correction of 4.51 kcal mol^{-1}. Note that the BSSE correction is within the range of 2.3~4.6 kcal mol^{-1} from previous calculations using similar levels of theory.[59] The calculated binding energy from this work is consistent with the previous theoretical data of 10.4 kcal mol^{-1} at the pseudopotential plane-wave DFT level of theory.[7] Moreover, the experimental binding energy of about 15 kcal mol^{-1} for water adsorbed on the perfect MgO surface can also provide a rough comparison with the present calculated value.[60]

Table 1. Selected optimized parameters (distances are in Å and angles in degrees) of water at the stationary points along the normal and surface healing dissociation pathways.

	Normal dissociation pathway		
	R	^{N}TS	^{N}P
Mg1–O5	2.27 (2.19)[a]	2.10	2.12 (2.12)[a] (2.11)[b]
Mg4–O5	3.96	2.94	2.12 (2.12)[a] (2.11)[b]
O2–H6	1.91	3.14	3.63
O5–H7	0.98 (0.97)[a]	1.23	2.32 (2.21)[b]
O5–H6	0.98 (0.99)[a]	0.97	0.96 (0.96)[a] (0.93)[b]
∢H6O5H7	102.7	106.1	76.0
∢Mg1O5H6H7	88.6	91.0	54.6

	Surface healing dissociation pathway			
	^{S}TS1	^{S}In	^{S}TS2	^{S}P
Mg1–O5	2.0	2.32	2.28	2.15
O5–H7	0.98	1.00	1.23	2.37
O5–H6	1.80	2.97	2.69	3.12
O2–H6	0.99	1.03	1.15	4.37
H6–H7	2.58	2.51	1.78	0.75
∢H6O5H7	133.9	54.2	32.9	0.49
∢Mg1O5H6H7	−114.9	−109.0	−109.6	−140.5

[a] Value is taken from reference [7]. [b] Value is taken from reference [41].

Dissociation of water on the vacancy site: In the present study we found that isolated water can dissociate on an oxygen vacancy of the MgO(100) surface via two separate pathways. One is referred to as the normal dissociation pathway as it has been found in previous theoretical studies.[7,41] In the second pathway the dissociation can also heal the surface and desorbs the hydrogen molecule and is referred to as the surface healing dissociation pathway. Selected geometrical parameters of stationary points along these two pathways are given in Table 1 (along with previous theoretical data) and are also shown in Figure 2. The energetic properties are listed in Table 2 and shown also in Figure 3.

Normal dissociation pathway: As shown in Figure 2a the normal dissociation pathway shows that the adsorbed water (R) near the vacancy dissociates into a proton that fills the vacancy and a hydroxyl that is bonded to two nearby magnesium atoms (^{N}P) via the transition state (^{N}TS). At the transition state (^{N}TS), the dissociated hydrogen atom (H7) is localized between the vacancy site and water oxygen atom, and the O5–H7 distance is 1.23 Å. The hydroxy group O5H6 is localized at the Mg1 atom tilting toward to the va-

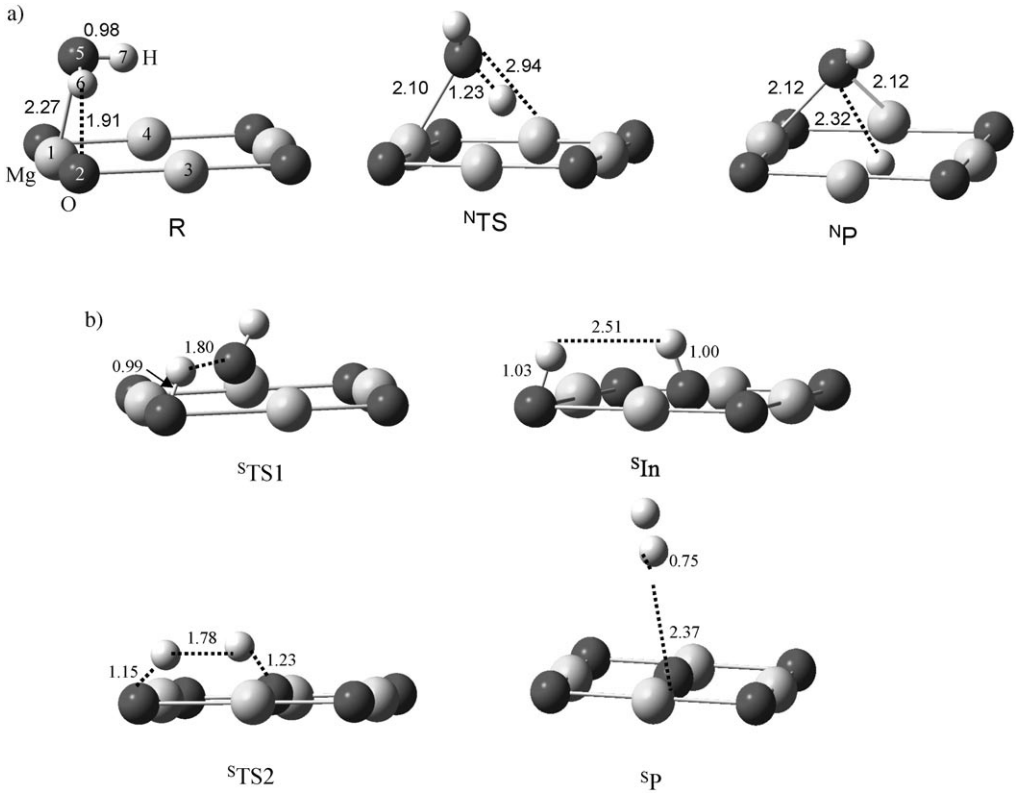

Figure 2. Optimized structures on the oxygen vacancy MgO(100) surface: a) for the normal dissociation pathway, b) for the surface healing dissociation pathway.

Table 2. Binding energies (E_{BD}), barrier heights ($\Delta V^{\neq}$) and reaction energies (ΔE) (kcal mol^{-1}) of water dissociation on an oxygen vacancy MgO(100) surface.

	Normal pathway		Surface healing pathway	
	B3LYP	IMOMO	B3LYP	IMOMO
E_{BD}	21.91	20.49	21.91	20.49
E_{BD}(ZPE+BSSE)	17.40	15.98	17.40	15.98
$\Delta V^{\neq}{}_{N}$	5.79	9.43	16.78	14.95
$\Delta V^{\neq}{}_{N}$(ZPE)	1.03	4.67	15.91	14.09
ΔE(reference to R)	−39.89	−48.20	−5.99	−7.69
ΔE(reference to R, ZPE)	−42.00	−46.09	−8.65	−10.34
$\Delta V^{\neq}{}_{S}$			4.72	10.75
$\Delta V^{\neq}{}_{S}$(ZPE)			−0.15	5.88
ΔE(reference to ^{S}In)			−76.21	−61.90
ΔE(reference to ^{S}In, ZPE)			−78.43	−64.12

cancy, and the Mg1−O5 distance is 2.10 Å. Normal-mode analysis confirms that ^{N}TS was the transition state corresponding to the dissociation of isolated water on the oxygen vacancy. The stable dissociated configuration of the product ^{N}P, in this pathway, corresponds to the oxygen atom (O5) of the hydroxy group (O5H6) bonded to two surface magnesium atoms (Mg1 and Mg4) for which the Mg−O distances are 2.12 Å. The dissociated proton (H7), which is located slightly below the surface plane by 0.18 Å, fills the vacancy site, and in this case the O5−H7 distance is 2.32 Å (see Figure 2a). The configuration of ^{N}P is similar to that found by Ahlswede et al.[41] and Finocchi et al.[7] as seen in Table 1. The bridge structure of the O5 atom bonded to two surface Mg atoms as well as the capture of H7 by the vacancy in ^{N}P play a rather active role in stabilizing this dissociated product (the hydroxyl and proton). In addition, the calculated frequency of 3850 cm^{-1} for the OH species of the product ^{N}P is somewhat higher than the IR experimental data of 3369 cm^{-1}.[61] The difference between the calculated and experimental frequency data indicates that the coadsorption water under experimental measurement conditions may reduce the bond strength of OH species.

The calculated forward barrier for this normal dissociation pathway is 4.67 kcal mol^{-1}, and the reaction energy relative to the adsorbed water (R) is −46.09 kcal mol^{-1} (see Table 2 and Figure 3). Our calculated results are slightly different from the estimated data of 7.29 kcal mol^{-1} and −38.05 kcal mol^{-1} using molecular dynamic simulations, respectively, reported by Finocchi et al.[7] The present results indicate that the dissociation of an isolated water molecule on an oxygen vacancy of the MgO(100) surface into a hydroxy group is feasible due to the small forward barrier along this pathway. Furthermore, the energy released from adsorption of the water molecule on the vacancy of 15.98 kcal mol^{-1} would provide energy for dissociation of the water to form ^{N}P. The large exoergicity of −46.09 kcal mol^{-1} would prevent the reverse reaction (reforming the water molecule) from occurring. Consequently, this dissociation pathway can explain the presence of a stable surface hy-

droxy group on the defective MgO surface in the limit of very low coverage in many experiments.[22,29,31]

Surface healing dissociation pathway: The surface healing pathway in which the dissociation of water may heal the oxygen vacancy and desorbs a hydrogen molecule is shown in Figure 2b. This pathway is quite different from that suggested by Finocchi et al.[7] from previous constraint MD simulations. The differences are discussed separately below. In our results, this pathway consists of first the hydrogen (H6) of water moving to the nearest neighboring surface oxygen (O2) to form a hydroxyl group, while the remaining hydroxy group of water fills the vacancy site to form the intermediate ^{S}In via a transition state ^{S}TS1; then two hydrogen atoms from the two hydroxy species formed in the first step in ^{S}In can recombine to form a hydrogen molecule above the surface plane via a transition state ^{S}TS2. The vacancy site is finally healed by the water oxygen atom. Selected optimized geometrical parameters are listed in Table 1. From Figure 2b and Table 1 it can be seen that in the transition state ^{S}TS1, the breaking H6 atom of water is almost bonded to the surface oxygen (O2) with a titling of the O2–H6 bond (0.99 Å) in the (110) direction; the remaining hydroxy group (O5H7) originally in water sits above the vacancy site by the oxygen atom (O5) bridging two surface magnesium atoms (Mg1 and Mg3) with a tilting of the O5–H7 bond (1.80 Å) also in the (110) direction. The angle of H6-O5-H7 expands from 102.7° in the adsorbed water structure (R) to 133.9° in ^{S}TS1. The intermediate ^{S}In has an orientation of two hydroxy species toward each other in the (110) direction, for which the O5–H7, O2–H6, and H6–H7 bond lengths of 1.00, 1.03, and 2.51 Å, respectively. Such orientation of two hydroxy species toward each other facilitates the following step of hydrogen recombination. The structure of the transition state ^{S}TS2 is close to that of the intermediate ^{S}In, except for the shorter distance of H6–H7 of 1.78 Å and the larger O5–H7 and O2–H6 bond lengths of 1.23 and 1.15 Å, respectively. In the product ^{S}P, the oxygen originally in the water molecule fills the vacancy site and the two hydrogen atoms form a hydrogen molecule (with a H–H bond length of 0.75 Å) molecularly adsorbed 2.37 Å above the surface. Normal-mode analysis confirmed that these TS states correspond to the surface healing dissociation pathway of an isolated water molecule on the oxygen vacancy MgO(100) surface. Note that although the oxygen atoms in O2–H6 and O5–H7 are represented by two different basis sets, for example O2(6–31G(d,p)) and O5(6–311G(d,p)), the effects of different split-valence basis sets on the geometries and relative energies were found to be small by Sushko et al.[15]

The calculated classical barriers for this pathway are shown in Figure 3 and Table 2. The first and second forward barriers are 14.09 and 5.88 kcal mol^{-1}, respectively, relative to the corresponding reactants, namely R and ^{S}In, respectively. The reaction energies relative to the adsorbed water molecule (R) are −10.34 and −74.46 kcal mol^{-1}, respectively. The latter value agrees well with the result reported by Finocchi et al (−73.7 kcal mol^{-1}).[7] The first dissociation barrier (14.09 kcal mol^{-1}) in this pathway is 1.90 kcal mol^{-1} below the energy of the separated water and surface. This suggests that dissociation of the water molecule via this pathway is possible. In addition, the classical barrier height of the rate-limiting step in the surface healing dissociation pathway is 9.32 kcal mol^{-1} higher than that of the normal dissociation pathway. This suggests that the water molecule dissociating into a hydroxy group along the normal dissociation pathway is energetically more favorable. These results support the fact that significant numbers of hydroxy groups from water dissociation have been detected by many experiments on the defective MgO surface.[22,29,31,61] On the other hand, the barrier for hydrogen formation from the intermediate ^{S}In of only 5.88 kcal mol^{-1} indicates that unless the intermediate ^{S}In is further stabilized by coadsorption of other water molecules as will be discussed below, it is possible to proceed to desorption of a hydrogen molecule and healing of the surface. Present results suggest that the dissociation of water on an oxygen vacancy on the MgO(100) surface can proceed by either or both of the two pathways. Depending on the experimental conditions, the existence of the surface healing dissociation mechanism may prevent the hydroxyl group from being detected by experiments such as in Goodman and co-workers's experiments.[31,32]

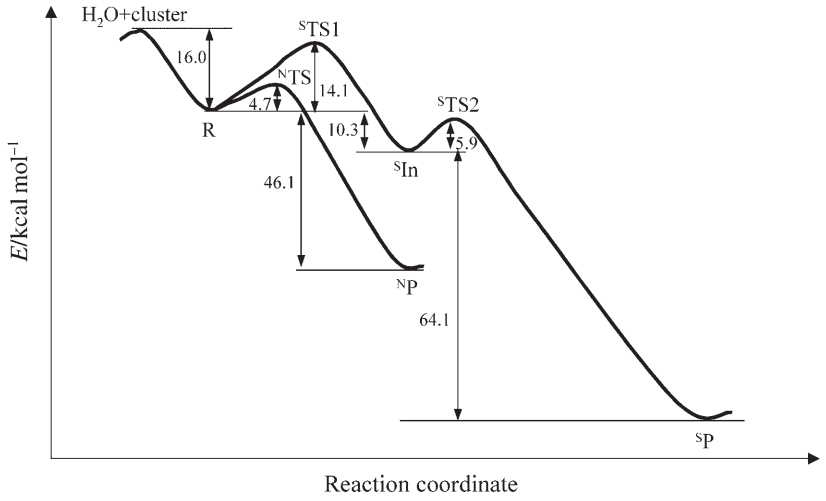

Figure 3. Schematic energy profiles for the normal and surface healing dissociation pathways on an oxygen vacancy on the MgO(100) surface. Relative energies are from IMOMO (CCSD:DFT/B3LYP) calculations.

The possibility for hydrogen formation and surface healing upon dissociation of a water molecule on an oxygen vacancy was first suggested by Finocchi et al.[7] However, the mechanism for such a process was found to be very different in our study. In the study by Finocchi et al., hydrogen formation is from the product of the normal dissociation pathway ^{N}P in which hydrogen formation occurs by abstraction of the hydrogen atom in OH along with the hydrogen in the vacancy. Thus, it is a subsequent step of the normal dissociation pathway. In our study, we found that hydrogen formation occurs along a separate pathway as discussed above. We have attempted to verify the hydrogen formation mechanism proposed by Finocchi et al., but we found that the hydrogen atom in the vacancy is rather stable and is not mobile and thus it is difficult to move it out of the vacancy to abstract the hydrogen atom of the OH group. We have made numerous attempts to locate a transition state for such a process but have failed.

Analysis of density of state spectra: To compare the calculated dissociation mechanism with the experimental results, we analyzed the electronic structure characteristics of the hydroxy species, which dissociated from the water molecule on the oxygen vacancy MgO surface. Figure 4 shows plots of the densities of states (DOS) based on the embedded B3LYP calculations along with the experimental results.[22] For a perfect surface, there are two peak groups in the valence band area that represent the surface oxygen and magnesium atoms (see Figure 4a). The surface oxygen vacancy induces a new peak around −2.5 eV in the bandgap, which is attributed to the excess surface electrons of the vacancy center (see Figure 4b). This result is consistent with the value calculated by Sushko et al.[15] After an isolated water

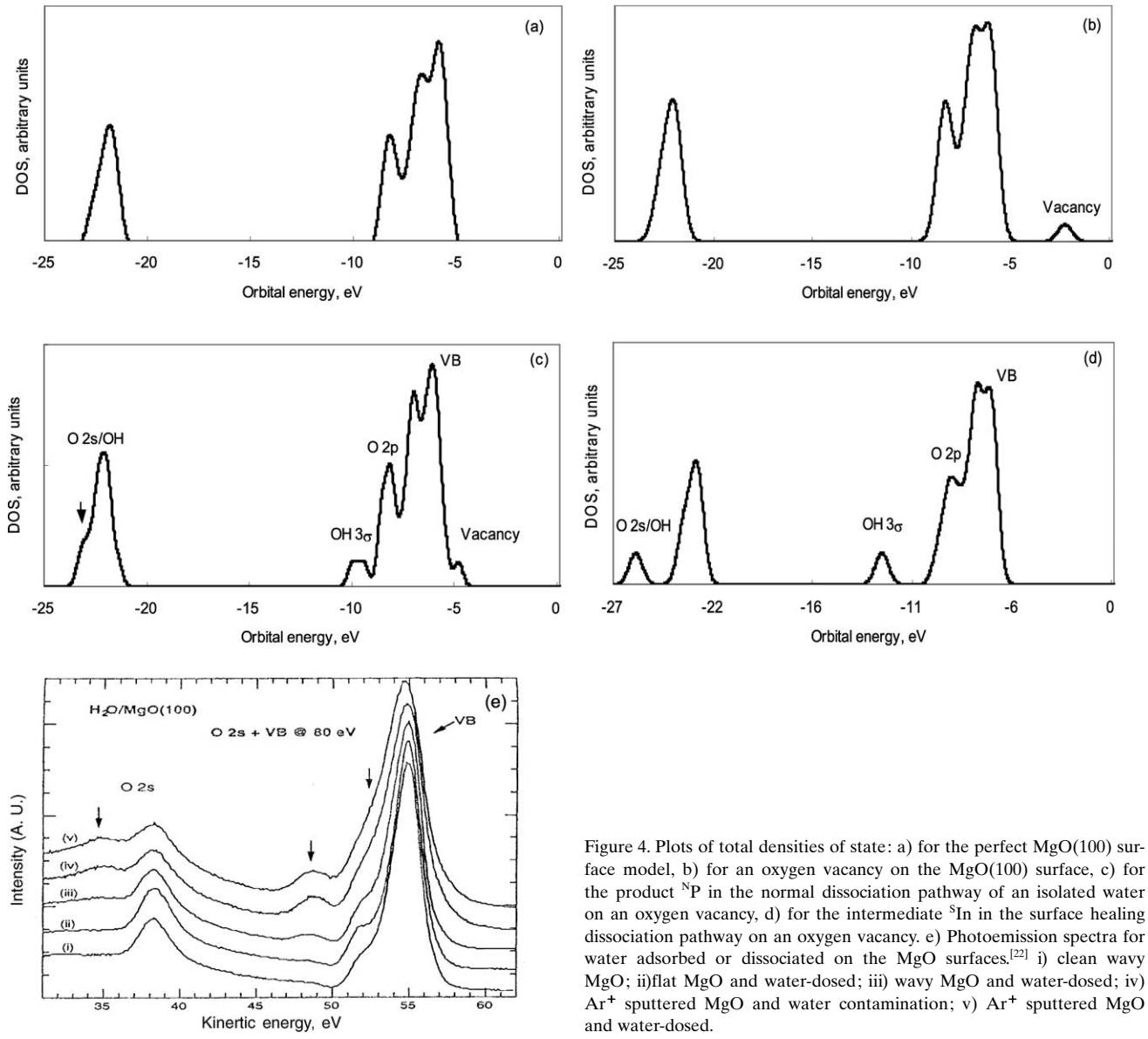

Figure 4. Plots of total densities of state: a) for the perfect MgO(100) surface model, b) for an oxygen vacancy on the MgO(100) surface, c) for the product ^{N}P in the normal dissociation pathway of an isolated water on an oxygen vacancy, d) for the intermediate ^{S}In in the surface healing dissociation pathway on an oxygen vacancy. e) Photoemission spectra for water adsorbed or dissociated on the MgO surfaces.[22] i) clean wavy MgO; ii)flat MgO and water-dosed; iii) wavy MgO and water-dosed; iv) Ar^{+} sputtered MgO and water contamination; v) Ar^{+} sputtered MgO and water-dosed.

dissociates to give a hydroxy group and a proton (^{N}P), two new peaks associated with the 2s orbital of oxygen and the σ-type orbitals of OH grow at −23.2 and −10.1 eV in product ^{N}P (see Figure 4c). The σ-type orbital population is attributed to the p orbitals of the oxygen atom and the s orbital of the hydrogen atom of the OH species. The vacancy peak moves to the surface atom band around −5 eV in ^{N}P, which implies that the excess electrons on the vacancy site transfer to the dissociated proton. It is further verified by a charge distribution analysis that the hydrogen charge distribution changes from +0.5 to −0.82 before and after the dissociation of water, respectively. The densities of states of ^{S}In in the surface healing dissociation pathway (see Figure 4d) show that two electron peaks around −25.6 and −12.5 eV represent the 2s orbital of oxygen and the σ-type orbitals of two OH species on the MgO surface, respectively. These two peaks in ^{S}In move down by about 2.4 eV, compared to those of ^{N}P in the normal dissociation pathway, which indicates that the H atoms connecting the surface O atoms in ^{S}In are different from the whole OH species localized above the MgO surface in ^{N}P. The calculated peak separations are given in Table 3 along with the experimental values from the photoemission spectra from Liu and co-workers shown in Figure 4e.[22] The calculated peak separations (see Table 3) between the O 2s peak of OH and the VB electronic peak, between the O 2s peak of OH and the 3σ peak of OH, and between the 3σ peak of OH and the VB electronic peak are 18.0, 13.2, and 4.8 eV for ^{N}P in the normal dissociation pathway, and 18.6, 13.1, and 5.5 eV for ^{S}In in the surface healing dissociation pathway, respectively, compared to the experimental values of 19.5, 13.5, and 6.0 eV.[22] It seems that the results from the surface healing pathway are in better agreement with experimental observation, because the discrepancies between the theoretical and experimental results on the peak separations of 0.9, 0.4, and 0.5 eV in the surface healing dissociation pathway are smaller than those of 1.5, 0.3, and 1.2 eV in the normal dissociation pathway. Comparing with the actual experimental spectra shown in Figure 4e, it is rather difficult to distinguish between these two types of hydroxy species in the ^{N}P and ^{S}In complexes. Consequently, it is possible to identify both of them in experiments. Therefore, this comparison further supports the interpretation of the photoemission spectra as evidence of water dissociation on the defective MgO(100) surface.

Table 3. Peak separations (eV) of electronic spectra of the product ^{N}P in the normal dissociation pathway and the intermediate ^{S}In in the surface healing dissociation pathway.

	Theory		Experiment[22]
	^{N}P	^{S}In	
O 2s/OH→VB	18.0	18.6	19.5
O 2s/OH → 3σ/OH	13.2	13.1	13.5
3σ/OH → VB	4.8	5.5	6.0

Coadsorptions of a water molecule near the vacancy: From our previous study,[42] one would expect that a coadsorbed water molecule can stabilize the hydroxy group in the case of the defective surface. To do so, we can estimate the degree of stabilization due to coadsorption of an additional water molecule along the dissociation pathways by calculating the energy profile using the same geometrical configurations as that of the isolated water, while optimizing the structure of the nearby coadsobed water molecule. The optimized structures of coadsorbed water and calculated energies are shown in Figure 5 and Figure 6 (dashed lines), respectively. From the structures of coadsorbed water near the dissociated water (Figure 5), we can conclude that hydrogen bonds between the hydroxy species and coadsorbed water molecule are formed in all calculated systems. These hydrogen bonds originating from the surrounding water would provide a driving force to stabilize the hydroxy species along the water dissociation pathways. The differences between the energy changes of the single water dissociation pathways and the energy profiles by adding one coadsorbed water molecule represent the degree of stabilization by the coadsorbed water along the two dissociation coordinates. We found that the coadsorbed water molecule stabilizes the adsorbed water (R) by 2.73 kcal mol^{-1}, ^{N}TS by 5.40 kcal mol^{-1}, and the dissociative hydroxy species ^{N}P by 8.25 kcal

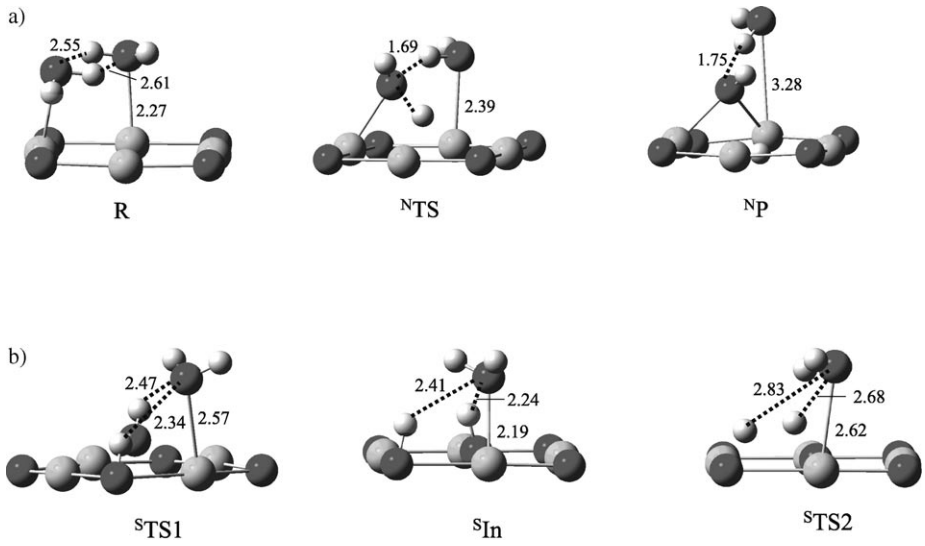

Figure 5. Optimized co-adsorbed water structures on the oxygen vacancy MgO(100) surface: a) for the normal dissociation pathway; b) for the surface healing dissociation pathway.

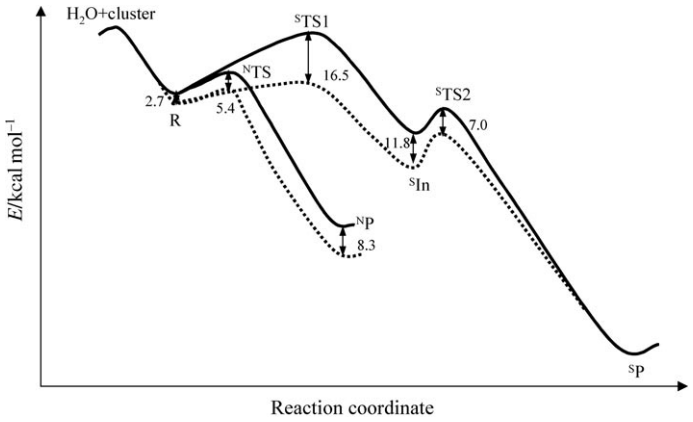

Figure 6. Energy change profiles (dashed lines) for the second water molecule coadsorbed near the original water molecule that retains its configuration in the isolated water dissociation pathways. Relative energies are from IMOMO (CCSD:DFT/B3LYP) calculations.

mol^{-1} in the normal dissociation pathway, and also lowers ^{S}TS1 by 16.50 kcal mol^{-1}, ^{S}In by 11.81 kcal mol^{-1}, and ^{S}TS2 by 6.97 kcal mol^{-1} in the surface healing dissociation pathway (see in Figure 6). It is expected that the degree of stabilization of the hydroxy group in the ^{N}TS, ^{N}P, ^{S}TS1, and ^{S}In complexes for adding more coadsorbed water molecules would facilitate the reaction processes by lowering the dissociation barriers of both pathways. This was also observed in our former study of the water dissociation on the perfect MgO(100) surface.[42] Furthermore, more coadsorbed water molecules would further stabilize the hydroxy species by forming additional hydrogen bonds with the two OH groups in the ^{S}In complex, and thus prevent the two hydrogen atoms from combining to form a hydrogen molecule. Note that the two OH species of the ^{S}In complex have six neighboring surface Mg atoms, which are the trapping sites of coadsorbed water molecules. A water molecule adsorbed at each of two Mg sites adjoined to two OH species can form two hydrogen bonds; a water molecule adsorbed at one of the other Mg sites can form one hydrogen bond. One can estimate that these eight potential hydrogen bonds with the two OH species can lead to a stabilization energy of about 48 kcal mol^{-1} for the ^{S}In complex, since the energy is lowered by about 6 kcal mol^{-1} for each hydrogen bond formed, as calculated in our work. Such stabilization can trap the OH species and prevent them from forming H_2 and healing the surface. Unfortunately, studying adsorptions of six coadsorbed water molecules would require a substantially larger MgO cluster to avoid edge effects and such calculations with the same level of theory are beyond our current computational capability. In summary, our results show that more coadsorbed water molecules would sufficiently facilitate the presence of OH species at a surface vacancy. In other words, the dissociation process of water on the MgO(100) surface occurs favorably at a surface oxygen vacancy to form surface OH species.

Conclusion

We have studied the interaction of a water molecule with an oxygen vacancy on the MgO(100) surface by using the DFT/B3LYP embedded cluster approach. We found that a water molecule initially adsorbs on one of the magnesium ions next to the vacancy site with a binding energy of 15.98 kcal mol^{-1}. Then the adsorbed water molecule can dissociate into two products through two different dissociation pathways. One dissociation pathway shows that the water molecule dissociates into a hydroxy species and a proton via a transition state with a forward barrier of 4.67 kcal mol^{-1}. The water dissociation along this reaction path is found to be energetically favorable, because the released energy (15.98 kcal mol^{-1}) from the water adsorbed on the surface overcomes this barrier easily. Moreover, the calculated overall reaction energy of -46.09 kcal mol^{-1} can further prevent the hydroxy species from reforming the water molecule spontaneously.

Another dissociation pathway indicates that the adsorbed water can produce a hydrogen molecule and an oxygen atom that heals the vacancy site via two transition states and an intermediate with a first barrier of 14.09 and a second barrier of 5.88 kcal mol^{-1}. The first barrier of this stepwise mechanism is close to the binding energy of adsorbed water with the surface, which predicts that the product of water dissociation on the defective MgO surface may also be the hydrogen molecule under certain experimental conditions, especially at higher temperature.

Analysis of the electronic spectra further confirms that the peaks located near -25 to -23 and -12 to -10 eV are due to the O 2s orbital and σ-orbital of the hydroxy species in the product including a hydroxy and a proton in the former pathway and in the intermediate with two OH species in the latter pathway, respectively. This thus supports the photoemission spectra interpretation of dissociation of water on the defective MgO(100) surface in the low water coverage range. It is expected that one water molecule coadsorbed near the vacancy would theoretically stabilize the hydroxy products by 8.25 and 11.81 kcal mol^{-1} in the two dissociation pathways, respectively. Coadsorption of more water molecules can further stabilize the hydroxy species on the surface and facilitate the water chemisorption process by lowering the barrier to dissociation. These dissociation mechanisms confirmed the observation of hydroxy species on the defective MgO(100) surface by previous experiments.

Acknowledgements

This work is supported by the National Science Foundation. We also acknowledge computing resources provided by the University of Utah Center for High Performance Computing.

[1] J. B. L. Martins, J. Andres, E. Longo, C. A. Taft, *Int. J. Quantum Chem.* **1996**, *57*, 861.

[2] A. C. Pavao, B. L. Hammond, M. M. Soto, W. A. Lester Jr., C. A. Taft, *Surf. Sci.* **1995**, *323*, 340.
[3] A. C. Pavao, M. M. Soto, W. A. Lester Jr., S. K. Lie, B. L. Hammond, C. A. Taft, *Phys. Rev. B* **1994**, *50*, 1868.
[4] J. B. L. Martins, E. Longo, J. G. R. Tostes, C. A. Taft, J. Andres, *J. Mol. Struct.* **1994**, *303*, 19.
[5] E. Longo, J. A. Varela, P. A. Marinho, V. C. Pandolfelli in *High Tech Ceramics* (Ed.: P. Vincenzini), Elsevier, New York, **1987**, p. 399.
[6] E. Longo, J. A. Varela, A. N. Senapeschi, O. J. Whittemore, *Langmuir* **1985**, *1*, 456.
[7] F. Finocchi, J. Goniakowski, *Phys. Rev. B* **2001**, *64*, 125426.
[8] E. A. Colbourn, *Surf. Sci. Rep.* **1992**, *15*, 281.
[9] A. L. Shluger, J. D. Gale, C. R. A. Catlow, *J. Phys. Chem.* **1992**, *96*, 10389.
[10] A. M. Ferrari, G. Pacchioni, *J. Phys. Chem.* **1995**, *99*, 17010.
[11] A. G. Pelmenschikov, G. Morosi, A. Gamba, S. Coluccia, *J. Phys. Chem.* **1995**, *99*, 15018.
[12] A. G. Pelmenschikov, G. Morosi, A. Gamba, S. Coluccia, *J. Phys. Chem. B* **1998**, *102*, 2226.
[13] E. Scorza, U. Birkenheuer, C. Pisani, *J. Chem. Phys.* **1997**, *107*, 9645.
[14] G. Pacchioni, P. Pescarmona, *Surf. Sci.* **1998**, *412/413*, 657.
[15] P. V. Sushko, A. L. Shluger, C. R. A. Catlow, *Surf. Sci.* **2000**, *450*, 153.
[16] B. Ealet, J. Goniakowski, F. Finocchi, *Phys. Rev. B* **2004**, *69*, 195413.
[17] L. Giordano, J. Goniakowski, J. Suzanne, *Phys. Rev. Lett.* **1998**, *81*, 1271.
[18] M. Odelius, *Phys. Rev. Lett.* **1999**, *82*, 3919.
[19] J. H. Cho, J. M. Park, K. S. Kim, *Phys. Rev. B* **2000**, *62*, 9981.
[20] L. D. Site, A. Alavi, R. M. Lynden-Bell, *J. Chem. Phys.* **2000**, *113*, 3344.
[21] E. Knozinger, K. H. Jacob, S. Singh, P. Hoffmann, *Surf. Sci.* **1993**, *290*, 388.
[22] P. Liu, T. Kendelewicz, G. E. Brown Jr., *Surf. Sci.* **1998**, *412/413*, 315.
[23] Y. D. Kim, R. M. Lynden-Bell, A. Alavi, J. Stulz, D. W. Goodman, *Chem. Phys. Lett.* **2002**, *352*, 318.
[24] D. Abriou, J. Jupille, *Surf. Sci.* **1999**, *430*, L527.
[25] C. A. Scamehorn, N. M. Harrison, M. I. McCarty, *J. Chem. Phys.* **1994**, *101*, 1547.
[26] C. A. Scamehorn, A. C. Hess, M. I. McCarty, *J. Chem. Phys.* **1993**, *99*, 2786.
[27] W. Langel, M. Parrinello, *Phys. Rev. Lett.* **1996**, *73*, 504.
[28] N. H. De Leeuw, G. W. Watson, S. C. Parker, *J. Phys. Chem.* **1995**, *99*, 17219.
[29] P. Liu, T. Kendelewicz, G. E. Brown Jr., G. A. Parks, *Surf. Sci.* **1998**, *412/413*, 287.
[30] Y. D. Kim, D. W. Goodman, *J. Phys. Chem. B* **2002**, *106*, 1515.
[31] M. A. Johnson, E. V. Stefanovich, T. N. Truong, J. Gunster, D. W. Goodman, *J. Phys. Chem. B* **1999**, *103*, 3391.
[32] J. Gunster, G. Liu, J. Stulz, S. Krischok, D. W. Goodman, *J. Phys. Chem. B* **2000**, *104*, 5738.
[33] M. A. Johnson, E. V. Stefanovich, T. N. Truong, *J. Phys. Chem. B* **1998**, *102*, 6391.
[34] M. J. Stirniman, C. Huang, R. S. Smith, S. A. Joyce, B. D. Kay, *J. Chem. Phys.* **1996**, *105*, 1295.
[35] M. A. Henderson, *Surf. Sci. Rep.* **2002**, *46*, 1.
[36] J. Goniakowski, C. Noguera, *Surf. Sci.* **1995**, *330*, 337.
[37] N. H. De Leeuw, S. C. Parker, *Phys. Rev. B* **1998**, *58*, 13901.
[38] K. Refson, R. A. Wogelius, D. G. Fraser, *Phys. Rev. B* **1995**, *52*, 10823.
[39] W. Langel, M. Parrinello, *J. Chem. Phys.* **1995**, *103*, 3240.
[40] J. A. Mejias, A. J. Berry, K. Refson, D. G. Fraser, *Chem. Phys. Lett.* **1999**, *314*, 558.
[41] B. Ahlswede, T. Homann, *Surf. Sci.* **2000**, *445*, 49.
[42] Y. Wang, T. N. Truong, *J. Phys. Chem. B* **2004**, *108*, 3289.
[43] A. Matveev, K. Neyman, I. Yudanov, N. Rosch, *Surf. Sci.* **1999**, *426*, 123.
[44] I. V. Yudanov, V. Nasluzov, K. Neyman, N. Rosch, *Int. J. Quant. Chem.* **1997**, *65*, 975.
[45] E. V. Stefanovich, T. N. Truong, *J. Phys. Chem. B* **1998**, *102*, 3018.
[46] E. V. Stefanovich, T. N. Truong, *J. chem. Phys.* **1996**, *104*, 22.
[47] P. L. Treesukol, T. N. Truong, *J. Phys. Chem. B* **2001**, *105*, 2421.
[48] V. Shapovalov, T. N. Truong, *J. Phys. Chem. B* **2000**, *104*, 9859.
[49] M. Svensson, S. Humbel, K. Morokuma, *J. Chem. Phys.* **1996**, *105*, 3654.
[50] S. Humbel, S. Seiber, K. Morokuma, *J. Chem. Phys.* **1996**, *105*, 1959.
[51] S. F. Boys, F. Bernardi, *Mol. Phys.* **1970**, *19*, 553.
[52] M. J. Frisch, G. W. Trucks, H. B. Schlegel, G. E. Scuseria, M. A. Robb, J. R. Cheeseman, V. G. Zakrzewski, J. A. Montgomery, Jr., R. E. Stratmann, J. C. Burant, S. Dapprich, J. M. Millam, A. D. Daniels, K. N. Kudin, M. C. Strain, O. Farkas, J. Tomasi, V. Barone, M. Cossi, R. Cammi, B. Mennucci, C. Pomelli, C. Adamo, S. Clifford, J. Ochterski, G. A. Petersson, P. Y. Ayala, Q. Cui, K. Morokuma, D. K. Malick, A. D. Rabuck, K. Ragha-Vachari, J. B. Foresman, J. Cioslowski, J. V. Ortiz, A. G. Baboul, B. B. Stefanov, G. Liu, A. Liashenko, P. Piskorz, I. Komaromi, R. Gomperts, R. L. Martin, D. J. Fox, T. Keith, M. A. Al-Laham, C. Y. Peng, A. Nanayakkara, M. Challacombe, P. M. W. Gill, B. Johnson, W. Chen, M. W. Wong, J. L. Andres, C. Gonzalez, M. Head-Gordon, E. S. Replogle, J. A. Pople, Gaussian 98, Revision A.7, Gaussian Inc., Pittsburgh PA, **1998**.
[53] Y. Wang, E. Florez, F. Mondragon, T. N. Truong, *Surf. Sci.* **2006**, in press.
[54] W. P. Unruh, J. W. Culvahouse, *Phys. Rev.* **1967**, *154*, 861.
[55] Z. X. Yang, R. Q. Wu, Q. M. Zhang, D. W. Goodman, *Phys. Rev. B* **2002**, *65*, 155407.
[56] M. C. Wu, C. M. Truong, D. W. Goodman, *Phys. Rev. B* **1992**, *46*, 12688.
[57] J. Kramer, C. Tegenkamp, H. Pfnur, *Phys. Rev. B* **2003**, *67*, 235401.
[58] L. A. Kappers, R. L. Kroes, E. B. Hensely, *Phys. Rev. B* **1970**, *1*, 4151.
[59] A. M. G. Ferrari, N. Rosch, U. Heiz, S. Abbet, A. Sanchez, G. Pacchioni, *J. Phys. Chem.* **2000**, *104*, 10612.
[60] S. Joyce, B. Kay, *J. Chem. Phys.* **1996**, *105*, 1295.
[61] M.-C. Wu, C. A. Estrada, J. S. Corneille, D. W. Goodman, *J. Chem. Phys.* **1992**, *96*, 3892.

Received: January 6, 2006
Published online: May 26, 2006

